A STUDY OF THE LINEAR AND NONLINEAR DYNAMICS OF A TROJAN ASTROPHYSICAL OBJECT WITHIN EXOPLANETARY SYSTEM HD 126053

AZEM HYSA[1], KLAUDIO PEQINI[2], MIMOZA HAFIZI[2]

[1]Applied and Natural Sciences Department, "Aleksander Moisiu"

University, Durres, Albania

[2]Department of Physics, Faculty of Natural Sciences,

University of Tirana, Albania

e-mail: azemhysa@gmail.com

Abstract

In many exoplanetary systems asteroids, planets, or moons can be found near Lagrange points L_4 and L_5. Described as many-body problems, planetary systems are fundamentally chaotic with high sensitivity from initial conditions. However, for various ranges of the mass parameter, there are observed specific regimes that defy chaoticity. Of particular relevance is the mass ratio parameter with critical value μ_c=0.0385. For this critical value, the stability of the Lagrange points L_4 and L_5 changes followed by a bifurcation of the system. The present paper focuses on analysing the motion of a test astrophysical objects within the exoplanetary system HD 126053. We aim to find a stable trajectory around the Lagrange points of an astrophysical object with application to the mentioned exoplanetary system. In the initial phase of the study we consider a body with utterly small mass (for example, the mass of a Trojan asteroid, Trojan exomoon, or the mass of a Trojan Earth planet) that begins it motion near one of the Lagrange points of the binary star system, HD 126053. In the second phase of the study we increase this mass until the critical value of the system's mass ratio is reached. We predict that an astrophysical object (or a cluster of astrophysical objects) with mass at most 6.365 M_J can orbit in a stable configuration around the Lagrange points within the HD 126053 system. The analytical calculations are performed under the framework of the Planar Circular Restricted Three-Body Problem. The studies about this problem and the results of this study are of great importance, especially in Physics, Astronomy, and the field of Mechanics of Celestial Bodies. On the other hand, they expand the applications of the theory of dynamical systems to better understand the dynamics of the interactions of celestial bodies in different exoplanetary systems.

Key words: *HD 126053 System, trojan earth lanet, trojan exomoon, trojan asteroid, lagrange points, circular restricted three-body problem.*

Përmbledhje

Në shumë sisteme ekzoplanetare, asteroidë, planetë ose hëna mund të gjenden pranë pikave të Lagranzhit L_4 dhe L_5. Të përshkruara si sisteme me shumë trupa, sistemet planetare janë thelbësisht kaotike me ndjeshmëri të lartë ndaj kushteve fillestare. Megjithatë, për vlera të ndryshme të prametrit të masës, vihen re zona specifike që sfidojnë kaoticitetin. Me rëndësi të vecantë është parametri i raportit të masës me vlerë kritike μ_c=0.0385. Për këtë vlerë kritike, stabiliteti i pikave të Lagranzhit L_4 dhe L_5 ndryshon dhe për pasojë ndodh një bifurkacion i sistemit. Artikulli aktual fokusohet në analizimin e lëvizjes së objekteve astrofizike test brenda sistemit ekzoplanetar HD 126053. Ne synojmë të gjejmë një trajektore stabël rreth pikave të Lagranzhit të një trupi astronomik në sistemin ekzoplanetar që përmendëm më sipër. Në fazën fillestare të studimit ne konsiderojmë një trup me masë krejtësisht të vogël (për shembull, masa e një asteroidi Trojan, ekzohëne Trojane, ose masa e një planeti Tokësor Trojanë) lëvizja e të cilit fillon në afërsi të njërës prej pikave të Lagranzhit të sistemit binar yjor, HD 126053. Në fazën e dytë të studimit rrisim vlerën e kësaj mase, derisa të arrihet vlera kritike e raportit të masës së sistemit. Ne parashikojmë që një objekt astrofizik (ose një grumbull objektesh astrofizike) me masë deri në vlerën 6.365 M_J mund të orbitojë në një konfigurim stabël përqark pikave të Lagranzhit brenda sistemit HD 126053. Llogaritjet analitike kryhen në kuadër të problemit të kufizuar rrethor planar të tre trupave. Studimet rreth këtij problemi dhe rezultatet e këtij studimi janë të një rëndësie të madhe, sidomos në Fizikë, Astronomi, dhe në fushën e Mekanikës së Trupave Qiellorë. Nga ana tjetër, ata zgjerojnë aplikimet e Teorisë së Sistemeve Dinamike për të kuptuar më mirë dinamikën e bashkëveprimeve të trupave qiellorë në sisteme të ndryshme ekzoplanetare.

Fjalë kyçe*: Sistemi HD 126053, ekzoplanet tokësor trojan, ekzohënë trojane. asteroid trojan, pikat e lagranzhit, problemi i kufizuar rrethor i tre trupave.*

Introduction

The case of two gravitationally interacting bodies can be fully solved, and was solved by Newton (Newton, 1687). The general three-body problem in Newtonian gravitation is fundamentally non-solvable from an analytical point of view (Liao et al., 2022; Li & Shijun, 2017) and the numerical solutions are quite complex to interpret (Li, Yipeng & Shijun, 2017). In order to gain valuable insights, simplified special cases are often analysed like the Circular Restricted Three-Body Problem (CRTPB). In this regime one of the three bodies, which has negligible mass, exerts a negligible force on the remaining bodies and virtually does not affect their motion (Haoze, 2019). Within this approximation, the study of the dynamics is reduced to the analysis of the motion of the third body revolving around two others already in Keplerian orbits around their common center of mass (Sirbu, Leonardi, 2023). A further simplification assumes the third body travels in the same plane as the two stars, thus yielding the Planar Circular Restricted Three-Body Problem (PCRTBP) (Bhanu, et.al, 2019).

The dynamics of a few bodies, particularly the Circular Restricted Three-Body Problem, is one of the intriguing topics in the subject of modern Nonlinear Mechanics and Dynamical Astronomy. Numerous areas of Astronomy, including Space Dynamics, Stellar Systems, Artificial Satellites, Stellar Cluster and Galactic Dynamics have employed the Circular Restricted Three-Body Problem which still represents an active and stimulating field of research (Kumar, Gupta, & Aggarwal, 2017; Zotos, 2015, Kumar, Kushvah, Kumar Pal, 2024).

In the case of two bodies where the much smaller one revolves around the more massive body, there exist five points called the Lagrange points and denoted by L_i, (i = 1, ..., 5). Among them, three are collinear (L_1, L_2, and L_3 (Euler 1763, 1764, 1765)) and two triangular (L_4, and L_5 (Lagrange, 1873)). A sketch of the Lagrange points is shown in Figure 1.

Often, mathematical models of real-world phenomena are formulated in terms of systems of nonlinear differential equations, which can be difficult to solve explicitly. To overcome this barrier, we take a qualitative approach to the analysis of solutions to nonlinear systems by making phase portraits (this is a geometric representation of the orbits of a dynamical system in the phase plane) and using Stability Analysis. To be able analyse these systems we will linearize them at their equilibria (Morgan, 2015). In this study, we use the Linear Stability Analysis and Nonlinear Analysis of the CRTBP.

The Linear Stability Analysis was used to study the stability of the Lagrange points. Linear Stability Analysis describes the behaviour of a system at near equilibrium (Demirel & Gerbaud, 2019). In our case, this equilibrium is the Lagrange points. Stability analysis based on the linearized CRTBP equations only guarantees that the system is stable to infinitesimal perturbations, but it may be unstable to finite ones (Chang & Lu, 2019). The collinear points are unstable for all values of mass parameter but triangular points are stable for the mass parameter under a critical value $\mu_c \approx 0.0385$ (Idrisi, Haruna, Eshetie, 2023). The fundamental theory of Nonlinear Analysis (a branch of mathematics (Zeidler, 1990) is to analyse a system's dynamics in phase space; a point in this region at any time characterizes the system's state.

This theory used to study the dynamics of nonlinear systems, chaos a deterministic system exhibits aperiodic behaviour that depends sensitively on the initial conditions, thereby rendering long-term prediction impossible (Strogatz, 2018), bifurcations, etc., and often relies on numerical methods and computational techniques to approximate solutions, as closed-form solutions may not be readily available. A bifurcation of a dynamical system occurs when the parameter value of a system changes such that it causes a sudden qualitative change in its behaviour (Caitlin Mc Cann, 2013).

The small orbits making small oscillations about equilibrium points (in our case about Lagrange points), traditionally called librations (Steven H. Strogatz, 2018). For orbits with relatively small eccentricities, the librations around the stable Lagrangian equilibrium points L_4 and L_5 are one of the two possible configurations of a stable co-orbital system, called a tadpole orbit (by analogy with the restricted three-body problem, determined L_4 as the equilibrium point when the less massive planet is 60^o ahead of the more massive one and L_5 when it is behind) (Hippke & Angerhausen, 2015, Leleu et al. 2015, 2017).

The first observation of a tadpole orbit was performed by Wolf (1906), where the asteroid Achilles shares its orbit with Jupiter around L_4. Today more than 6000 bodies (Jupiter Trojans) in tadpole orbits are known, as well as a few other cases involving Neptune, Mars, and Earth (Leleu et al. 2015, Marzari et al. 2002).

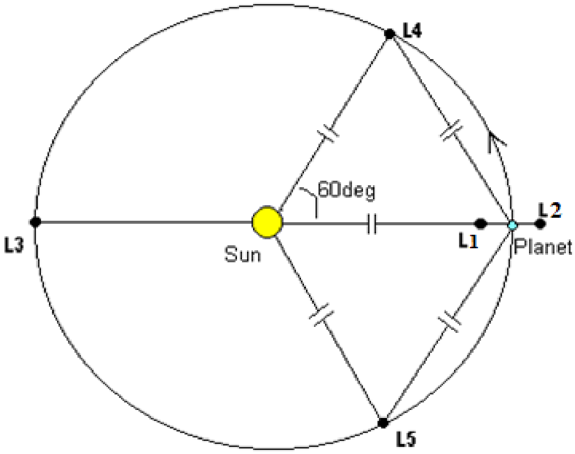

Figure 1. Schematic representation of Lagrange points for the Sun-Earth system (Image source:

https://www.spaceacademy.net.au/library/notes/lagrangp.htm).

Here we are interested on co-orbital configurations, the configurations of two or more astronomical bodies (such as asteroids, moons, or planets) orbiting at the same, or very similar, distance from their primary star. Several celestial bodies in co-orbital configurations exist in our solar systems. However, co-orbital exoplanets have not yet been discovered (Leleu et al. 2015), due to the challenges such observations pose. A potential observation of co-orbital exoplanets would provide valuable information on the formation of planetary systems as well as on the interactions between planets and their host star (Robutel & Leleu, 2024).

Some interesting results are presented in three articles by Hysa, nonlinear dynamics of a test particle near the Lagrange points L_4 and L_5 (Earth-Moon and Sun-Earth case) (Hysa, 2024), a study of the nonlinear dynamics inside the exoplanetary system Kepler-22 using MATLAB® software (Hysa, 2024a) and study of the resonant motion of a test particle inside Kepler 69 using Circular Restricted Three-Body Problem (Hysa, 2024b). Presuming the existence of Trojan astronomical bodies within exoplanetary systems, we employ the Circular Restricted Three-Body Problem model in the binary star system HD 126053, which has been selected from among several tens such systems for the reasons outlined below. This system is composed of a primary star (HD 126053 A) with a mass of 0.89 M_S and a secondary star (HD 126053 B) with a mass of 0.03 M_S, where M_S is the solar mass. The mass parameter of this system is approximately 0.0326, less than the critical value μ_c. An additional reason for our emphasis on this binary system is its proximity to our solar system, located at a distance of 57.08 light years, which enhances the likelihood of direct observations.

Methods

In this study, we use the Circular Restricted Three-Body Problem model. This model describes the motion of a celestial body with negligible mass in three-dimensional physical space (Stephanie et al. 2019). The motion is governed by the gravitational attraction of two massive bodies, which are assumed to rotate in circles with uniform angular velocity around their common center of mass (Murray & Dermott, 1999). The two massive bodies (primary and secondary) have masses m_1 and m_2 ($m_1 \geq m_2$), respectively. The third body with mass m_3 has a negligible effect on the motions of m_1 and m_2 (Stephanie et al. 2019, Blaga et al., 2021). In CRTBP, the mass ratio (Yan, 2020, Langford & Lauren M. Weiss 2023):

$$\mu = \frac{m_2}{m_1+m_2}, \tag{1}$$

determines the dynamical solution (Langford A., and Lauren M. Weiss 2023).

We set the center of mass of the system as the origin and we set the position of m_1 at $(-\mu, 0, 0)$, and the position of m_2 at $(1-\mu, 0, 0)$ (Yan, 2020). From Kepler's third law we have $T^2 = 4\pi^2 a^3/G(\mu_1 + \mu_2)$, where $\mu_1 = 1-\mu$ and $\mu_2 = \mu$. In our calculations, the unit of distance a is the distance between primary and secondary star. The unit of time is taken such that the period of the orbits of primary and secondary stars is $T = 2\pi$ and the universal constant of gravitation becomes $G = 1$ (Langford, & Lauren M. Weiss 2023). Under these assumptions the equations of motions for the CRTBP in the nondimensional form read (Gheorghe Sirbu, Mauro Leonardi, 2023):

$$\begin{aligned} \ddot{x} &= 2\dot{y} + \frac{\partial U}{\partial x}. \\ \ddot{y} &= -2\dot{x} - \frac{\partial U}{\partial y}. \\ \ddot{z} &= \frac{\partial U}{\partial z}, \end{aligned} \tag{2}$$

where x, y, and z are the components of the third body relative to the system barycenter (Murray & Dermott, 1999) and $\dot{x} = v_x$, $\dot{y} = v_y$, and $\dot{z} = v_z$ are the velocity components of the third body, according to the directions x, y, and z, respectively. The pseudo-potential function U is given by

$$U = \frac{1}{2}(x^2 + y^2) + \left(\frac{1-\mu}{r_1} + \frac{\mu}{r_2}\right) + \frac{\mu(1-\mu)}{2}, \quad (3)$$

where $r_1 = \sqrt{(x+\mu)^2 + y^2 + z^2}$ and $r_2 = \sqrt{(x+\mu-1)^2 + y^2 + z^2}$ are the distances from the primary and secondary star to the third body, respectively (Korneev & Aksenov, 2020). The CRTBP has one integral of motion, namely the energy E:

$$E = \frac{(\dot{x}^2+\dot{y}^2+\dot{z}^2)}{2} + U = -\frac{C}{2}, \quad (4)$$

Astronomers also often use the *Jacobi constant* $C = -2E$ (Yan, 2020, Langford, & Lauren M. Weiss 2023).

Considering that the dynamical equation of the third body in the Circular Restricted Three-Body Problem is a time-varying high-dimensional non-linear system in the inertial frame, it can hardly be solved by using analytical approaches (Fabao Gao & Yongqing, 2020).

Nonlinear systems can be very complicated, if not impossible, to solve explicitly; however, when it comes to modelling real-world phenomena, the majority of the systems that arise are nonlinear. To be able to analyze these systems we will linearize them at their equilibria, and then construct phase portraits to visualize the trajectories of the solutions to the system (Morgan, 2015).

The analytical solution of the nonlinear system (2) is unknown (Korneev & Aksenov, 2020). So, the generation of trajectories of an astronomical test body requires the use of numerical methods. For the numerical integration of this nonlinear system, we used the Runge–Kutta–Fehlberg method (RKF45). This method is an algorithm in the Numerical Analysis that can be used to solve numerically the nonlinear system (2) (Sharmin et al., 2021, Svetlana, 2017, John H. Mathews & Kurtis K. Fink, 2004).

Some particular solutions obtained by the Linearization Method can give restricted analytical solutions (Korneev & Aksenov, 2020). This method (Linearization Method) is a linear approximation of the nonlinear system (2) that is valid in a small region around Lagrange points.

The problem of the stability condition in the linear approximation of the Lagrange points L_4 and L_5 was first studied by Gascheau in 1843. They found that if the co-orbital astronomical bodies were in circular and coplanar motion, the Lagrange points would be linearly stable if:

$$\frac{m_1 m_2 + m_1 m_3 + m_2 m_3}{(m_1+m_2+m_3)^2} < \frac{1}{27}. \quad (5)$$

For the Circular Restricted Three-Body Problem, we can define the mass parameter by equation (1). Some results from this problem are expected to hold in the non-restricted case. To compare our results with the restricted case we define the mass parameter in our system as:

$$\mu_3 = \frac{m_2+m_3}{m_1+m_2+m_3}, \quad (6)$$

which is a generalization of the mass parameter considered in the restricted case (Leleu, et al. 2015, Moraes et al., 2023). So, from this parameter, we have the possibility to consider the mass of the third body in the calculations.

We introduce the state vector $\mathbf{x} = [x, y, z, \dot{x}, \dot{y}, \dot{z}]^T$ and its time derivative $\dot{\mathbf{x}} = [\dot{x}, \dot{y}, \dot{z}, \ddot{x}, \ddot{y}, \ddot{z}]^T$ (Truesdale, 2012). Substituting the acceleration terms from the system of equations (2), we see that $\dot{\mathbf{x}}$ is a function of $\mathbf{x}$:

$$\dot{\mathbf{x}} = \frac{d\mathbf{x}}{dt} = \begin{pmatrix} \dot{x} \\ \dot{y} \\ \dot{z} \\ 2\dot{y} + \frac{\partial U}{\partial x} \\ -2\dot{x} + \frac{\partial U}{\partial y} \\ \frac{\partial U}{\partial x} \end{pmatrix} = A\mathbf{x}, \quad (7)$$

where

$$A = \frac{\partial \dot{\mathbf{x}}}{\partial \mathbf{x}} = \begin{pmatrix} 0 & 0 & 0 & 1 & 0 & 0 \\ 0 & 0 & 0 & 0 & 1 & 0 \\ 0 & 0 & 0 & 0 & 0 & 1 \\ U_{xx} & U_{xy} & U_{xz} & 0 & 2 & 0 \\ U_{yx} & U_{yy} & U_{yz} & -2 & 0 & 0 \\ U_{zx} & U_{zy} & U_{zz} & 0 & 0 & 0 \end{pmatrix}, \quad (8)$$

- is the Jacobian of the state derivative $\dot{\mathbf{x}}$ and U_{xx}, U_{xy}, U_{xz}, U_{yx}, U_{yy}, U_{yz}, U_{zx}, U_{zy}, and U_{zz} are the second-order partial derivatives of U given by Equation (3) (Langford & Lauren M. Weiss, 2023; Truesdale, 2012). Given a matrix A, if $Av = \lambda v$, v is an eigenvector and λ the corresponding eigenvalue. The system $(A - \lambda I)v = 0$ has a non-trivial solution (i.e. $v \neq 0$) if and only if $\det(A - \lambda I)v = 0$(Nipoti, 2018). When $\det(A - \lambda I)v = 0$ is written explicitly, it is a polynomial in λ, known as the characteristic polynomial of the matrix (Nipoti, 2018). For the Planar Circular Restricted Three-Body Problem ($z = 0$), the linear stability of points L_4 and L_5 is treated in many textbooks, e.g. Murray and Dermott (1999). The proper frequencies λ in the vicinity of triangular points are solutions of:

$$\lambda^4 + \lambda^2 + \frac{27}{4}\mu(1-\mu) = 0. \quad (9)$$

The frequencies of motion of a celestial body around L_4 and L_5 are given by Murray and Dermott (1999):

$$\begin{aligned} \lambda_{1,2} &= \pm\sqrt{\tfrac{1}{2}\left[-1-\sqrt{1-27\mu(1-\mu)}\right]}, \\ \lambda_{3,4} &= \pm\sqrt{\tfrac{1}{2}\left[-1+\sqrt{1-27\mu(1-\mu)}\right]}, \end{aligned} \quad (10)$$

where $\lambda_{1,2}$ is the frequency of the short–period epicyclic motion and $\lambda_{3,4}$ is the frequency of the long-period motion epicenter about L_4 or L_5.

The concept of stability applies in general to $\mathbf{x}(t)$, which is a solution of a system of differential equations $\dot{\mathbf{x}} = \mathbf{f}(\mathbf{x}, t)$. *Stability of equilibrium points*: $\mathbf{x} = \mathbf{L}$, where $\mathbf{L} = const$, is a stable equilibrium point if, for given $\gamma > 0$, there exist an $\delta > 0$ such that if at a reference (initial) time t_0, $|x(t_0)| - \mathbf{L} < \delta$ then, for all $t > t_0$, $|x(t)| - \mathbf{L} < \gamma$ (Nipoti, 2018). An equilibrium point is *linearly stable* if it is stable against all small (i.e. linear) disturbances ($|\delta\mathbf{x}|/|\mathbf{x}| \ll 1$). An equilibrium point is *non-linearly stable* if it is stable all disturbances (not necessarily small). In general, linear stability does not imply non-linear stability, but it has been shown that for $\mu < \mu_c$ the triangular points are also non-linearly stable (Nipoti, 2018).

Results and discussions

The data in Table 1 are taken from the links: https://www.stellarcatalog.com/, https://adg.univie.ac.at/schwarz/multiple.html,https://exoplanetarchive.ipac.caltech.edu/docs/counts_detail.html,https://www.stellarcatalog.com/stars/hd-126053.

We have determined the mass parameter for 136 binary star systems, as shown in Table 1. Given that the mass the third body in proximity to the Lagrange points is negligible, we ascertain the mass parameter for each system. For HD 126053, we have $m_1 = 0.89 M_S$ and $m_2 = 0.03\ M_S$. Substituting these values in equation (1), and we have $\mu = 0.0326$, slightly less than the critical value

μ_c. Additionally, we identify five other systems with a mass parameter that falls below this critical value.

Table 1. Some exoplanetary systems (Binary Star Systems) and their mass parameter (https://www.stellarcatalog.com/, https://adg.univie.ac.at/schwarz/multiple.html,https://exoplanetarchive.ipac.caltech.edu/docs/counts_detail.html,https://www.stellarcatalog.com/stars/hd-126053).

Nr.	Exoplanetary system name	Primary mass (M_S)	Secondary mass (M_S)	Mass parameter μ	Distance from the Sun (ly)
1	15 Sagittae	1.1200	0.0660	0.0556	58.00
2	HD 145825	1.0300	0.0600	0.0550	73.00
3	HD 149825	1.0300	0.0600	0.0550	826.0
4	HD 72946	0.9700	0.0660	0.0637	83.82
5	HD 194667	0.9600	0.0670	0.0652	104.4
6	HIP 70849	0.6300	0.0500	0.0735	79.00
7	EPIC 247589423 (K2-136)	0.7400	0.1000	0.1190	194.0
8	HD 177830	1.0700	0.7600	0.1370	205.0
9	Luhman 16	0.0320	0.0270	0.4576	6.500
10	Gliese 54	0.4300	0.3000	0.4110	26.90
11	Kepler 14	1.5100	1.3900	0.4790	3196
12	Kepler 1647	1.2200	0.9700	0.4430	3961
13	Kepler 34	1.0480	1.0210	0.4930	4889
14	Kepler 35	0.8880	0.8090	0.4770	5365
15	Gliese 747	0.4000	0.4000	0.5000	27.00
16	Gliese 185	0.5900	0.3700	0.3854	27.00
17	HD 180617	0.4500	0.0780	0.1480	19.28
18	2 MASS J18352-3123	0.2000	0.1000	0.3333	27.00

19	HD 188015	1.0900	0.2100	0.1610	32.00
20	Sirius	2.0630	1.0180	0.3304	8.700
21	TYC 398-1081-1	0.7000	0.2000	0.2222	28.00
22	HD 189733	0.8000	0.2000	0.2000	63.60
23	Gliese 618	0.4000	0.2000	0.3333	28.00
24	HD 190360	1.0400	0.2000	0.1610	52.00
25	WASP 85	1.0900	0.8800	0.4470	32.00
26	WASP 94	1.2900	1.2400	0.4900	647.0
27	HD 97101	0.6500	0.5400	0.4540	38.78
28	GJ 676 AB	0.7100	0.1700	0.1930	53.65
29	GJ 86 AB	0.8000	0.4900	0.3800	35.55
30	HD 101930	0.7400	0.6700	0.4740	99.44
31	XO-2	0.9800	0.9800	0.5000	489.2
32	HD 106515	0.9100	0.8800	0.4920	114.8
33	FW Tauri AB	0.2800	0.2800	0.5000	472.9
34	g Cephei Ab B	1.1800	0.3200	0.2130	44.98
35	GJ 3021 Ab B	0.9000	0.1300	0.1260	57.47
36	GJ 338 AB	0.5910	0.5960	0.4980	20.65
37	HD 106906	1.3000	1.3000	0.5000	300.1
38	Gliese 65 (Luyten 726-8)	0.1220	0.1160	0.4874	8.741
39	HD 222259	1.0100	0.8400	0.4540	143.9
40	HD 109271	1.0500	0.6000	0.3640	182.6
41	Chi 1 Orions	1.0290	0.1500	0.1272	28.00
42	HD 114762	0.8400	0.1380	0.1410	128.7
43	Gliese 3454	0.2000	0.1300	0.3939	28.00

44	HD 116029	1.5800	0.2600	0.1410	401.8
45	61 Cygni	0.7000	0.6300	0.4737	11.42
46	HD 13167	1.3500	0.2100	0.1350	32.00
47	HD 142	1.2000	0.5900	0.3300	67.18
48	HD 142022	0.9900	0.6000	0.3770	117.0
49	Procyon	2.0500	0.6020	0.2270	11.40
50	HD 16141	1.0100	0.2860	0.2210	117.1
51	HD 1666	1.5000	0.3600	0.1940	385.8
52	Struve 2398	0.3340	0.2700	0.4470	11.50
53	HD 176071	1.0700	0.7600	0.4150	48.89
54	Gliese 250	0.8000	0.5000	0.2174	29.00
55	HD 195019	1.0600	0.6970	0.3970	121.8
56	HD 196885	1.3300	0.5500	0.2930	107.6
57	Groombridge 34	0.3980	0.1600	0.2867	12.00
58	HD 197037	1.1100	0.3400	0.2350	107.6
59	Gliese 745	0.3520	0.3480	0.4971	29.00
60	HD 19994	1.3400	0.3500	0.2070	72.99
61	HD 202772	1.6900	1.2100	0.4170	480.1
62	SCR 1845-6357	0.0700	0.0300	0.3000	13.00
63	HD 20782	1.0000	0.8400	0.4570	117.5
64	LDS 169	0.4000	0.4000	0.5000	29.00
65	HD 212301	1.2700	0.3500	0.2160	171.9
66	HD 19994	1.3400	0.3500	0.2070	72.99
67	Kruger 60	0.2710	0.1760	0.3937	13.00
68	Ross 614	0.2230	0.1110	0.3323	13.00
69	FL Virginis	0.1430	0.1310	0.4781	14.00

70	HD 202772	1.6900	1.2100	0.4170	480.1
71	HD 20782	1.0000	0.8400	0.4570	117.5
72	Gliese 15	0.3800	0.1500	0.2830	11.74
73	HAT-P-32 AB	1.1760	0.4000	0.2540	1044
74	55 Cnc Ab-fB	0.9500	0.1300	0.1200	42.46
75	DP Leo AB	0.6900	0.0900	0.1150	1304
76	HAT-P-33 AB	1.4030	0.5600	0.3840	1366
77	HD 212301	1.2700	0.3500	0.2160	171.9
78	Gliese 412	0.4800	0.1000	0.1724	16.00
79	HD 213240	1.2200	0.1460	0.1070	132.9
80	70 Ophiuchi	0.9000	0.7000	0.4375	17.00
81	HD 217786	1.0200	0.1600	0.1360	181.3
82	El Cancri	0.1100	0.1000	0.4762	17.00
83	HD 222582	0.9900	0.3000	0.2330	137.0
84	Stein 2051	0.6800	0.2200	0.2444	18.00
85	HD 233832	0.7100	0.4200	0.3720	192.4
86	Gliese 752	0.4600	0.0750	0.1402	19.00
87	Eta Cassiopeiae	0.9720	0.5700	0.3696	19.00
88	Furuhjelm 46	0.3200	0.2900	0.4754	19.00
89	279 G. Sagittari	0.6500	0.2400	0.2697	20.00
90	HD 23472	0.7500	0.1400	0.1570	127.5
91	QY Aurigae	0.2260	0.1920	0.4593	20.00
92	EQ Pegasi	0.4360	0.1710	0.2817	20.00
93	HD 238090	0.5780	0.2300	0.2850	49.70
94	Gliese 338	0.6900	0.6400	0.4812	21.00
95	HD 27442	1.2000	0.7500	0.3850	59.03

96	Xi Bootis	0.8810	0.7000	0.4428	22.00
97	HD 30856	1.3500	0.5400	0.2860	429.0
98	Gliese 229	0.1550	0.0286	0.1558	22.00
99	HD 38529	1.4800	0.3000	0.1690	138.0
100	Gliese 829	0.2700	0.2700	0.5000	22.00
101	HD 39855	0.8200	0.5300	0.3930	75.89
102	Scholz	0.0950	0.0630	0.3987	22.00
103	Gliese 880	0.5860	0.2000	0.2545	22.00
104	LHS 6167	0.1300	0.1000	0.4348	24.00
105	HD 4113	0.9900	0.5500	0.3570	137.0
106	Gliese 831	0.2200	0.1200	0.3529	24.00
107	HD 42936	0.8700	0.0800	0.0840	153.0
108	HU Delphini	0.2370	0.1140	0.3248	24.00
109	HD 46375	0.9100	0.5800	0.3890	96.50
110	Gaia DR2 6702242043883732864	0.1000	0.1000	0.5000	25.00
111	HD 4732	1.7400	0.5300	0.2340	189.0
112	HD 5278	1.1260	0.3000	0.2100	32.00
113	Gliese 3991	0.5000	0.2000	0.2857	25.00
114	Mu Cassiopeiae	0.7400	0.1700	0.1868	25.00
115	Gliese 623	0.5100	0.0600	0.1053	26.00
116	Gliese 257	0.2500	0.2400	0.4898	26.00
117	Chi Draconis	1.0290	0.7300	0.4150	26.00
118	p Eridani	0.8800	0.8600	0.4943	27.00
119	WISE 1217+1626	0.0190	0.0110	0.3667	29.00
120	FK Aquarii	0.4200	0.4200	0.5000	29.00

121	Gama Leporis	1.2300	0.8200	0.4000	29.00
122	WT 460	0.1000	0.0800	0.4444	30.00
123	Gliese 283	0.6200	0.2000	0.2439	30.00
124	WISE 0458+6434	0.0143	0.0130	0.4762	30.00
124	Gliese 1103	0.0950	0.0640	0.4025	30.00
125	SDSS J1416+1348	0.0720	0.0300	0.2941	30.00
126	66 G. Centauri	0.8890	0.4000	0.3103	30.00
127	Wolf 1062	0.3700	0.1700	0.3148	31.00
128	Gliese 3253	0.1670	0.0500	0.2304	32.00
129	Gliese 680	0.4000	0.3000	0.4286	32.00
130	289 G. Hydrae	0.8700	0.0800	0.0842	31.00
131	**HD 165131**	1.0600	0.0178	0.0165	188.8
132	**HD 47127**	1.0200	0.0200	0.0192	87.08
133	**HN Pegasi**	1.0850	0.0270	0.0243	59.03
134	**HD 97334**	1.1000	0.0350	0.0308	74.04
135	**Gliese 758**	0.9660	0.0300	0.0314	50.88
136	**HD 126053**	0.8900	0.0300	0.0326	57.08

For $\mu_3 < \mu_c$, we have stable trajectories for an astrophysical object around the Lagrange points. Substituting the values $m_1 = 0.89 M_S$, $m_2 = 0.019\ M_S$ and $m_3 = 6.365\ M_J$ ($M_J = 1.898 \times 10^{27}$ kg is the mass of Jupiter) in equation (5), we find $\mu_3 = \mu_c = 0.0385$. So, the eigenvalues (Equations (10)) for this case are: $\lambda_{1,2} = \pm 0.7071i$ and $\lambda_{3,4} = \pm 0.7071i$. From these results we see that the eigenvalues are purely imaginary and the sum of all eigenvalues is zero. So, the Lagrange points L_4 and L_5 are neutrally stable fixed points. For $m_3 > 6.365\ M_J$, we have $\mu_3 > \mu_c$, and the Lagrange points are unstable. Thus, if $\mu_c < \mu < 0.5$, then L_4 and L_5 are unstable (Gabern & Jorba, 2001).

Sicardy (2010) shows that between μ_c and $\mu \approx 0.039$ the L_4 and L_5 points are globally stable in the sense that a particle released at those points at zero velocity (in the co-rotating frame) remains in the vicinity of those points for an indefinite time. Also, he shows elsewhere that there exists a family of stable periodic orbits surrounding L_4 or L_5 for $\mu \geq \mu_c$ (Fawzy & Abd El-Salam, 2012). The global stability of these points has been studied by several authors, such as Leontovich (1962), Deprit and Deprit-Barthlomé (1967), Markeev (1969), Szebehely (1979), Narayan and Ramesh (2008), Singh (2011) and Shankaran et al., etc. (2011). Their final conclusion is that in the planar case, the Lagrange points L_4 and L_5 are always stable within some domain of mass ratio (mass parameter) which is modified when including such kinds of different perturbations (Fawzy & Abd El-Salam, 2012).

The linearized system characteristic equation (9) processes four complex roots and a bifurcation at $m_3 = 6.365\ M_J$ (see Figure 2). This corresponds to the critical value of the mass parameter of the system, $\mu_c = 0.0385$. For $\mu < \mu_c$, the linearized system has distinct eigenvalues lying on the imaginary axis $\lambda = \pm i\omega_1, \pm i\omega_2$ where $0 < \omega_2 < \frac{\sqrt{2}}{2} < \omega_1 < 1$. As the mass parameter approaches μ_c, these imaginary eigenvalues converge into a pair of identical eigenvalues (see Equations (10) at the critical point where $\mu = \mu_c$. Finally, for $\mu > \mu_c$, the eigenvalues become complex and are symmetric about the imaginary axis such that some of the eigenvalues include a positive real part $\lambda = \pm a \pm ib$ (Duffy, 2012).

Now the main purpose of this paper is to numerically integrate the nonlinear system (2) and we will present the results in the phase plane. The phase plane is important for studying nonlinear systems. The phase plane is a method for visualizing the characteristics of these systems, and it is a two-dimensional case of the three-dimensional phase space.

Figures 3 – 6 show several trajectories around the Lagrange points L_4 and L_5 for different values of the mass of an astrophysical object near these points. Initial conditions in the nondimensional form for the coordinate and velocity are: $x_0 = 0.484$; $y_0 = 0.855$; $z_0 = 0$ and $\dot{x}_0 = v_{x0} = 0$; $\dot{y}_0 = v_{y0} = 0.0059$; $\dot{z}_0 = v_{z0} = 0$, respectively. For all the cases presented in these Figures, we used these initial conditions. The only change we made was the mass of the third body, to see how the trajectory of this body changes in the phase plane. This is the reason why we keep the same initial conditions for the coordinate and velocity. We take these initial conditions to have non-chaotic orbits around the Lagrange points L_4 and L_5. If these initial conditions change very little, then the orbits become chaotic. Figure 3, presents the positions of the Lagrange points L_4 and L_5 (in blue and red, respectively), and the positions of the two stars, HD 126053 A and HD 126053 B (in yellow and pink, respectively). Also, this Figure shows two nonlinear orbits around the Lagrange points L_4 and L_5 for $m_3 = M_E$, where M_E is the mass of the Earth.

Figure 4 shows two nonlinear trajectories around the Lagrange points L_4 and L_5 for $m_3 = M_J$. From the numerical experiment, we see that these configurations are stable for a very long time of integration. We can also present this result in the phase plane (x, v_x), and (y, v_y), respectively, as in Figure 5.

Figure 6 shows two nonlinear orbits around the Lagrange points L_4 and L_5 for $m_3 = 6.365M_J$ (in this case we have $\mu_3 = \mu_c$). In this case, we are not sure if this configuration will be stable for a very long time. However, from a numerical experiment we performed for a relatively large integration time, we see that this configuration was stable. Figure 7 shows a nonlinear trajectory around the Lagrange points L_5 for $m_3 = 8.22\ M_J$ (in this case we have $\mu_3 > \mu_c$). This configuration is not stable, but the orbit around L_5 becomes spiral and the third body moves away from the gravitational field of the HD 126053 system.

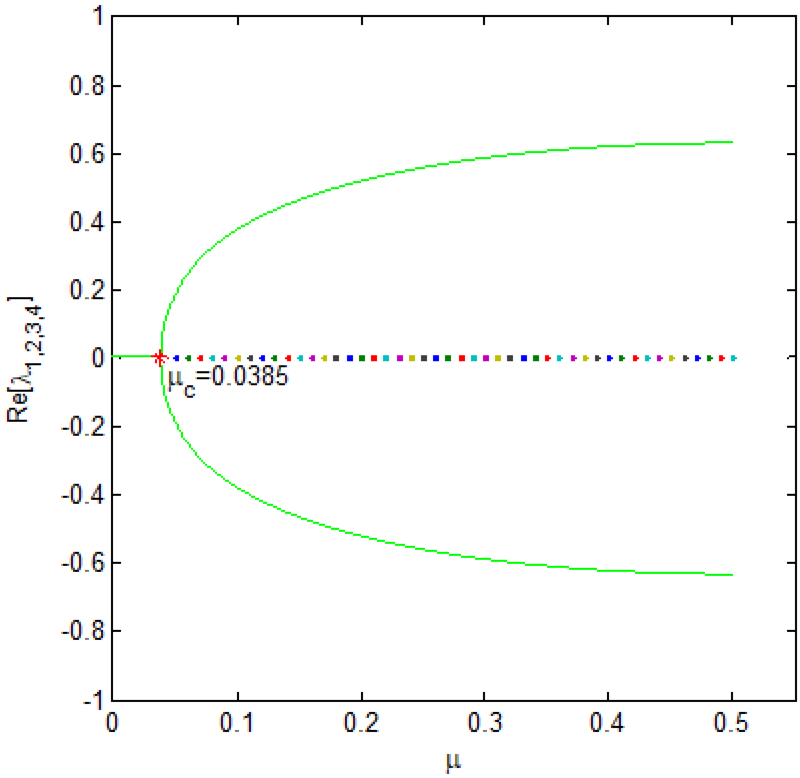

Figure 2. Bifurcation of the HD 126053 system for $\mu_3 = \mu_c = 0.0385$.

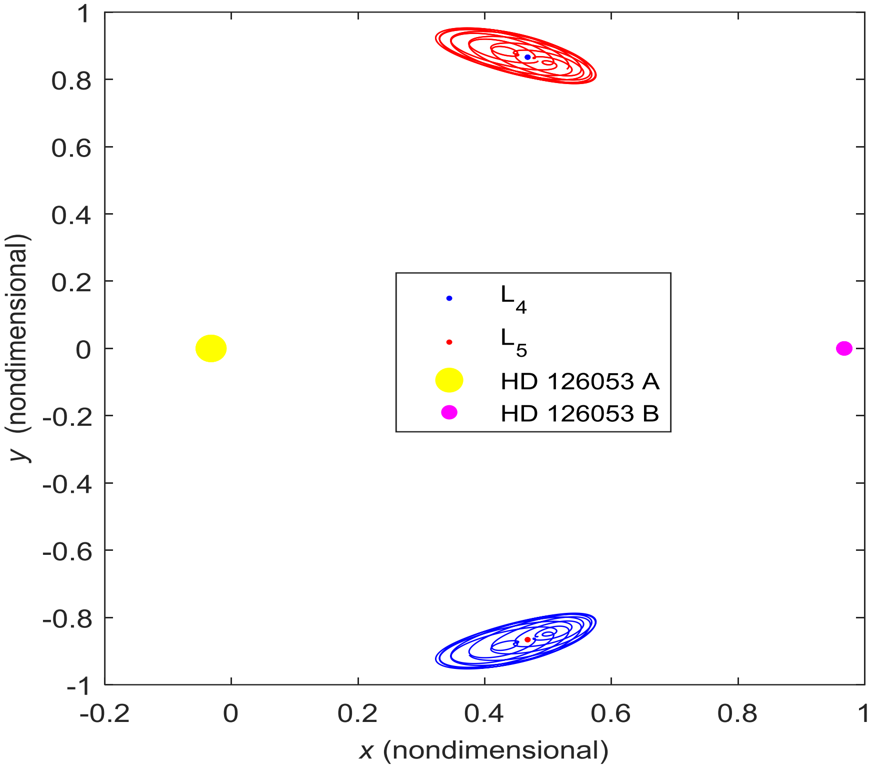

Figure 3. Nonlinear stable orbits around the Lagrange points L_4 and L_5 of an astrophysical object with the mass of a terrestrial planet.

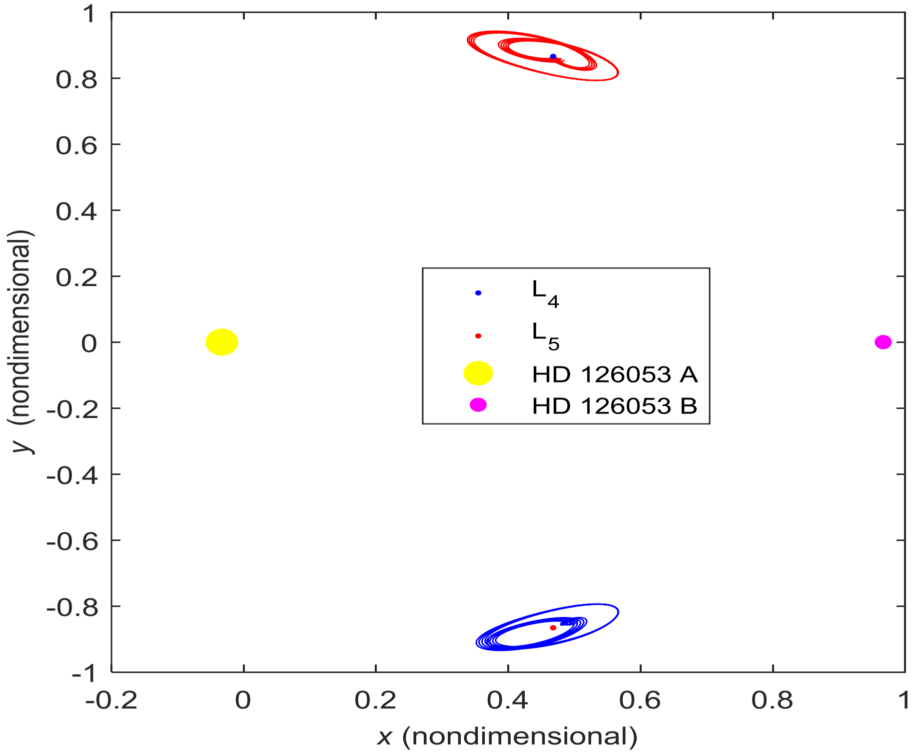

Figure 4. Nonlinear stable orbits around the Lagrange points of an astrophysical object for $m_3 = M_J$.

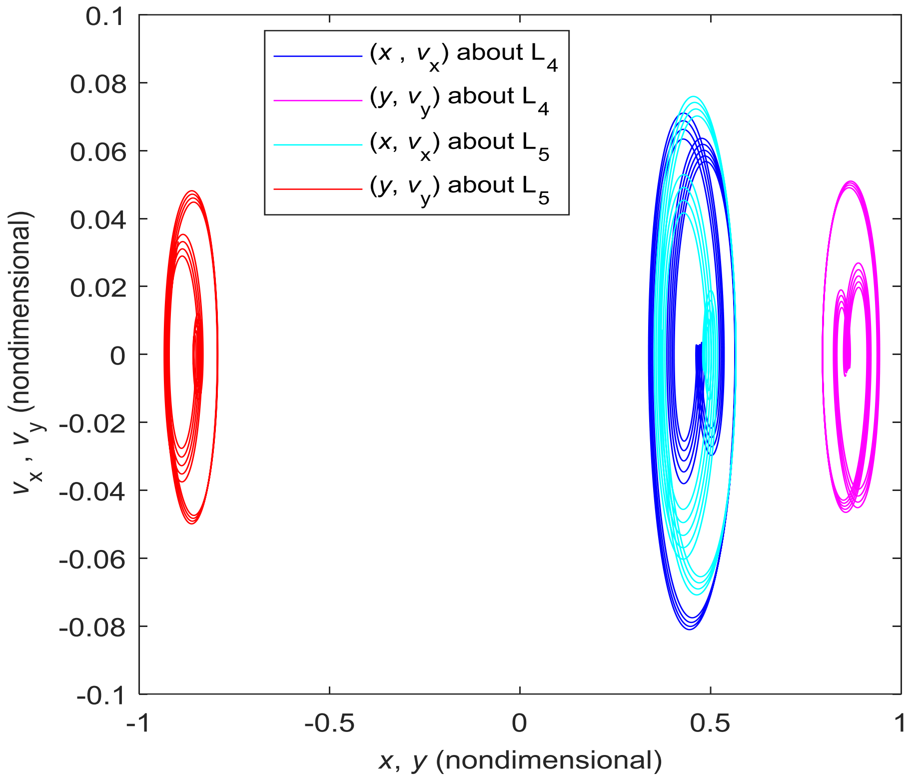

Figure 5. Phase-plane about L_4 and L_5.

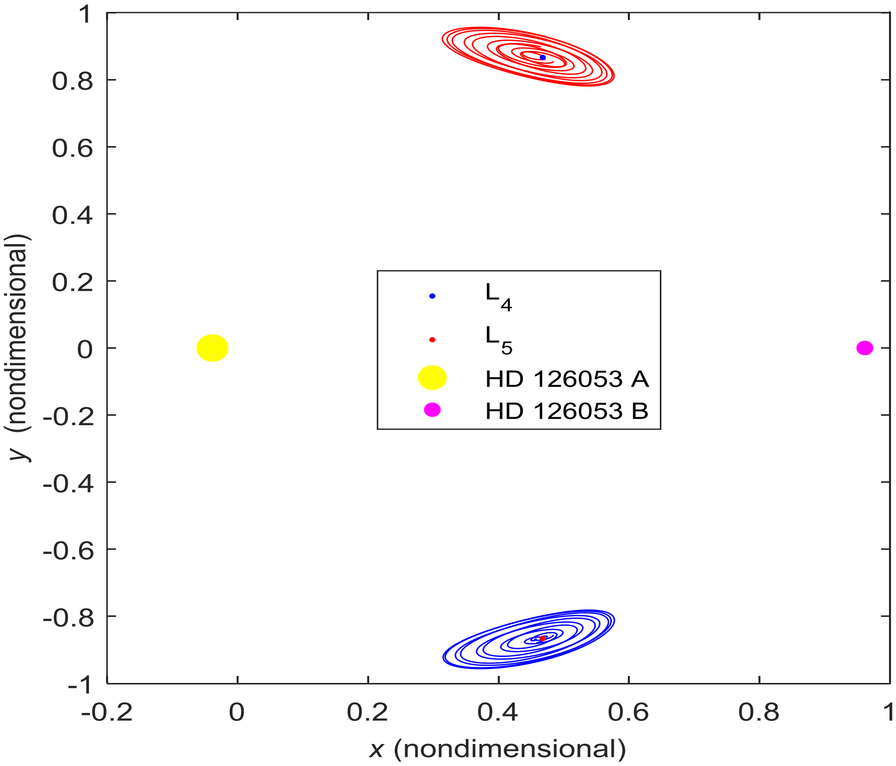

Figure 6. Nonlinear stable orbits around the Lagrange points of an astrophysical object with mass $m_3 = 6.365\ M_J$.

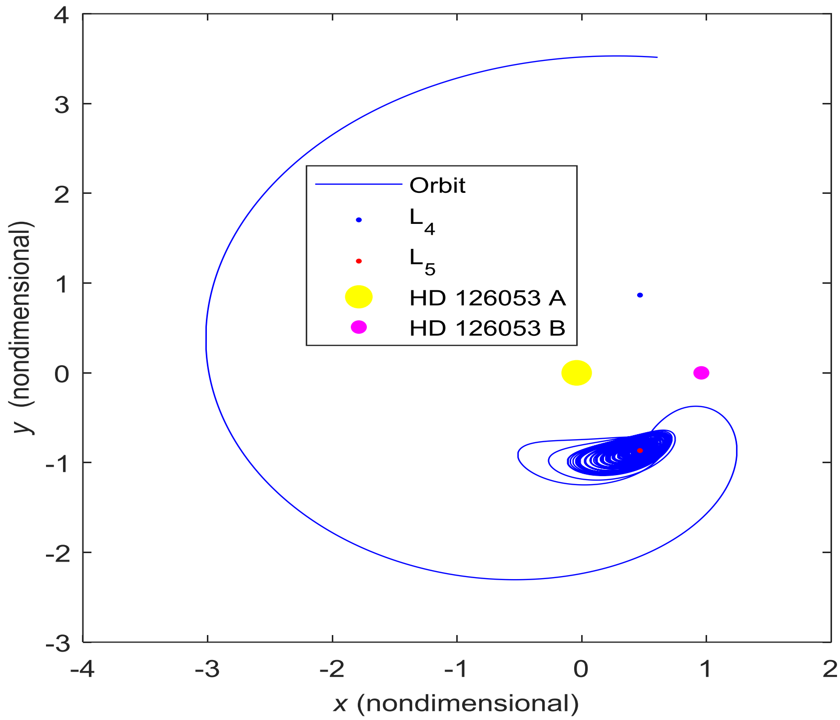

Figure 7. Nonlinear unstable orbit around L_5 of an astrophysical object with mass $m_3 = 8.22\ M_J$.

These results and the study of the nonlinear dynamics around the Lagrange points L_4 and L_5 are very important and can help us better understand the dynamics of the movement of celestial bodies in the HD 126053 system.

Conclusions

In this study, we have analysed the binary star system **HD 126053**, which has a mass parameter very close to μ_c. By calculating the mass parameter for 136 binary star systems, we observed that only six of them have this parameter smaller than μ_c. Thus, in these six binary star systems we expect astronomical objects in stable orbits around the respective Lagrange points L_4 and L_5. These systems are: **HD 126053**, **Gliese 758**, **HD 97334**, **HN Pegasi**, **HD 47127**, **HD 165131**. No celestial body has yet been discovered in any of these systems, and we predict that in one of them there is a high chance to observe such stable trajectories.

Through current instruments, it is difficult to detect celestial bodies such as exomoons, extrasolar comets, rings around exoplanets, and trojan astrophysical objects near the Lagrange points L_4 and L_5 in exoplanetary systems. Therefore, in this study, based on the model of the Circular Restricted Three Body Problem, Linear Stability Analysis, and Nonlinear Stability Analysis we strongly believe in the existence of stable trajectories of trojans around the Lagrange points within at least one of the above-mentioned exoplanetary systems. We calculate the mass of this astrophysical object (group of Trojan astrophysical objects) is from a very small Trojan asteroid to $6.365\ M_J$. This large mass can be detected with conventional methods, thus increasing the possibility for an imminent discovery in the near future.

This study constitutes a contribution to the domain of exoplanetary dynamics, providing original insights into the motion of celestial bodies within the **HD 126053** system near to the Lagrange points L_4 and L_5.

Contributions of the authors

The contributions of the first author are: study conception, data collection, writing code in MATLAB® Software and performing calculations, analysis and interpretation of results, wrote the paper and manuscript preparation.

The contribution of the second author is the control of the calculations and the manuscript.

The contribution of the third author resides primarily in the recommendation of the astrophysical objects that are central in this research.

Acknowledgment

The authors would like to thank Professors: Margarita Ifti and Dode Prenga for their suggestions.

References

Bhanu K., Rodney L. Anderson, Rafael de la Llave (2019), High-Order Resonant Orbit Manifold Expansions for Mission Design in the Planar Circular Restricted 3-Body Problem, 70th International Astronautical Congress, Washington D.C., United States, 21-25 October 2019.

Blaga et al., 2021, Jacobi Stability Analysis of the Classical Restricted Three Body Problem. http://arxiv.org/abs/2104.02432v1.

Caitlin McCann (2013). Bifurcation Analysis of Non-linear Differential Equations. University of Liverpool. http://www.maths.liv.ac.uk/~bnvasiev/Past%20students/Caitlin_399.pdf.

Chang, L., Lu, D. (2019), Stabilization of Lagrange points in circular restricted three-body problem: A port-Hamiltonian approach. Volume 383, Issue 16, pp. 1907-1914.

Demirel, Y., Gerbaud, V. (2019): Nonequilibrium Thermodynamics, Transport and Rate Processes in Physical, Chemical and Biological Systems. Fourth Edition, 2019. Chapter 12– Stability analysis. pp. 573-602.

Deprit, A. and A. Deprit-Bartholome, (1967). Stability of the triangular lagrangian points. Astron. J., 72: 173-179.

Duffy, B., (2012) "Analytical Methods and Perturbation Theory for the Elliptic Restricted Three-Body Problem of Astrodynamics", May 20, 2012.

Euler, L.: Considerationes de motu corporum coelestium. Novi Commentarii Academiae Scientiarum Petropolitanae 10, 544 (1764).

Euler, L. : Considérations sur le problème des trois corps. Mém. de Lacad. d. Sc. de Berlin 19, 194 (1763).

Euler, L.: De motu rectilineo trium corporum se mutuo attrahentium. Novi Commentarii Academiae Scientiarum Petropolitanae 11, 144 (1765).

Fabao Gao & Yongqing Wang, Approximate Analytical Three-Dimensional Multiple Time Scales Solution to a Circular Restricted Three-Body Problem. Advances in Astronomy. Volume 2020, Article ID 8868137, 10 pages.

Fawzy A, Abd El-Salam, (2012) "Discovery of an Equilibrium Circle in the Circular Restricted Three Body Problem", American Journal of Applied Sciences 9 (9): 1378-1384, 2012 ISSN 1546-9239 © 2012 Science Publication.

Gabern F., and A. Jorba, A., (2001) "A restricted four-body model for the dynamics near the lagrangian points of the sun-jupiter system", Discrete and continuous, Volume 1, Number 2, May 2001.

Gascheau G., (1843) C. R. Acad. Sci. Paris, 16, 393.

Gheorghe Sirbu, Mauro Leonardi (2023). Fully Autonomous Orbit Determination and Synchronization for Satellite Navigation and Communication Systems in Halo Orbits. Remote Sens. 15, 1173.https://doi.org/10.3390/rs15051173.

Haoze T., (2019). Koopman Reduced Order Control for Three-Body Problem. Modern Mechanical Engineering, 9, 20-29 http://www.scirp.org/journal/mme ISSN Online: 2164-0181 ISSN Print: 2164-0165.

Hippke M., and Angerhausen, D., (2015), A Statistical Search for A Population of Exo-Trojans In the Kepler Data Set, The Astrophysical Journal, 811:1 (5pp), 2015 September 20, http://dx.doi.org/10.1088/0004-637X/811/1/1.

https://adg.univie.ac.at/schwarz/multiple.html.

https://exoplanetarchive.ipac.caltech.edu/docs/counts_detail.html.

https://www.spaceacademy.net.au/library/notes/lagrangp.htm.

https://www.stellarcatalog.com/.

https://www.stellarcatalog.com/stars/hd-126053.

Hysa, A. (2024). Non-linear dynamics of a test particle near the Lagrange points L4 and L5 (Earth-Moon and Sun-Earth case). EUREKA: Physics and Engineering, (1), 3-10. https://doi.org/10.21303/2461-4262.2024.002949.

Hysa, A. (2024a). A study of the nonlinear dynamics inside the exoplanetary system Kepler-22 using MATLAB® software. *EUREKA: Physics and Engineering*, (2), 3-12. https://doi.org/10.21303/2461-4262.2024.003257.

Hysa, A. (2024b). Study of the resonant motion of a test particle inside Kepler 69 using circular restricted three body problem. *Technology Transfer: Fundamental Principles and Innovative Technical Solutions*, 34-37. https://doi.org/10.21303/2585-6847.2024.003563.

Idrisi, J., M., Haruna, S., Eshetie, T. (2023), Noncollinear equilibrium points in CRTBP with Yukawa – like corrections to Newtonian potential under an oblate primary model. Advances in Astronomy, Volume 2023, Article ID 4932794, 11 pages. https://doi.org/10.1155/2023/4932794.

John H. Mathews and Kurtis K. Fink (2004). Numerical Methods Using Matlab, 4th Edition, ISBN: 0-13-065248-2.

Korneev A., and Aksenov S., (2020), Calculation of libration point orbits in the circular restricted three-body problem. Journal of Physics: Conference Series 1740 (2021) 012019 IOP Publishing doi:10.1088/1742-6596/1740/1/012019.

Kumar, R., Kushvah, B., S., Kumar Pal A., (2024), Dynamics of the perturbed restricted three-body problem with quantum correction and modified gravitational potential. Archive of Applied Mechanics (2024) 94:651-665. http://dx.doi.org/10.1007/s00419-024-02543-3.

Kumar, V., Gupta B., R., & Aggarwal R., (2017). Numerical Simulation of the Phase Space of Jupiter-Europa System Including the Effect of Oblateness. Vol. 12, Issue 1, pp. 479 – 495.

Lagrange, J.L. : Essai sur le problème des trois corps, 229. In: Serret, J.-L. (ed.) Œuvres de Lagrange, Tome sixième, Gauthier-Villard, Paris (1873).

Langford A., and Lauren M. Weiss (2023). A Dynamical Systems Approach to the Theory of Circumbinary Orbits in the Circular Restricted Problem. ArXiv:2302.00580v1 [astro-ph.EP] 1 Feb 2023. https://doi.org/10.48550/arXiv.2302.00580.

Leleu, A., Robuetel, P., Correia A. C. M. and Lillo-Box, J. (2015), Detectability of quasi-circular co-orbital planets. Application to the radial velocity technique, A&A 581, A128 (2015).

Leleu, A., Robuetel, P., Correia A. C. M., and Lillo-Box, J. (2017), Dedection of co-orbital planets by combining transit and radial-velocity measurements, A&A 599, L7 (2017). https://doi.org/10.1051/0004-6361/201630073.

Leontovich, A.M., 1962. On the stability of the restricted problem of three bodies. Soviet math. Dokl., 3: 425-428.

Li X., Shijun L., (2017). More than six hundred new families of Newtonian periodic planar collisionless three-body orbits". Science China Physics, Mechanics & Astronomy. Vol. 60 No.

12: 129511 doi: 10.1007/s11433-017-9078-5. http://dx.doi.org/10.1007/s11433-017-9078-5 .

Li X., Yipeng J., and Shijun L. (2017), The 1223 new periodic orbits of planar three-body problem with unequal mass and zero angular momentum. arXiv:1709.04775v1 [nlin.CD] 13 Sep 2017. https://doi.org/10.48550/arXiv.1709.04775.

Liao at al., 2022. Three-body problem - from Newton to supercomputer plus machine learning, New Astronomy 96, 101850. http://arxiv.org/abs/2106.11010v2.

Markeev, A.P., 1969. On the stability of the triangular libration points in the circular bounded three-body problem. J. Applied Math. Mech., 33: 105-110. DOI: 10.1016/0021-8928(69)90117-8.

Marzari, F., Scholl, H., Murray, C., et al. 2002, in Origin and Evolution of Trojan Asteroids, ed. W. F. Bottke (Tucson: Univ. Arizona Press).

Moraes et al., 2023. The Dynamics of Co-orbital Giant Exomoons - Applications for the Kepler-1625 b and Kepler-1708 b Satellite Systems. arXiv:2301.10730v2 [astro-ph.EP] 27 Jan 2023.

Morgan, Robert (2015) "Linearization and Stability Analysis of Nonlinear Problems," Rose-Hulman Undergraduate Mathematics Journal: Vol. 16: Iss. 2, Article 5. Available at: https://scholar.rose-hulman.edu/rhumj/vol16/iss2/5.

Murray C., D., and Dermott. S., F., 1999, Solar System Dynamics. Cambridge University Press, 1st edition, 1999. ISBN: 0521 57295 9.

Narayan, A. and C. Ramesh, 2008. Stability of triangular points in the generalized restricted three body problem. J. Mod. Ex-B, France.

Newton, I (1687). Philosophiæ naturalis principia mathematica (Mathematical Principles of Natural Philosophy). London: Royal Society Press, 1687.

Nipoti, C., 2018, The circular restricted three body problem, Celestial Mechanics, Universita di Bologna (2018).

Robutel P., and Leleu A. (2024), Trojan Exoplanets, arXiv:2402.15168v1 [astro-ph.EP] 23 Feb 2024.

S. H. Strogatz (2018). Nonlinear Dynamics and Chaos with Applications to Physics, Biology, Chemistry, and Engineering.

Shankaran, S., J.P. Sharma and B. Ishwar, 2011. Equilibrium points in the generalised photogravitational non-planar restricted three body problem. Int. J. Eng., Sci. Technol., 3: 63-67.

Sharmin et al., 2021. A Study on Numerical Solution of Initial Value Problem by Using Euler's Method, Runge-Kutta 2 nd Order, Runge-Kutta 4th Order, and Runge-Kutta Fehlberg Method with MATLAB. International Journal of Scientific & Engineering Research Volume 12, Issue 3, March-2021 ISSN 2229-5518. https://www.researchgate.net/publication/376799308.

Sicardy, B., (2010). Stability of the triangular Lagrange points beyond Gascheau's value. Celest Mech Dyn Astr (2010) 107:145–155 DOI 10.1007/s10569-010-9259-5.

Singh, J., 2011. Nonlinear stability in the restricted three-body problem with oblate and variable mass. Astrophys Space Sci., 333: 61-69. DOI: 10.1007/s10509-010-0572-y.

Stephanie et al. 2019, Rendezvous Strategies in the Vicinity of Earth-Moon Lagrangian Points. Frontiers in Astronomy and space Sciences. ORIGINAL RESEARCH published: 22 January 2019 https://doi.org/10.3389/fspas.2018.00045.

Svetlana, G., (2017). Appendix A Runge-Kutta Methods (PDF). Munster Institute for Theoretical Physics. pp. 8–11. Retrieved 4 March 2022.

Szebehely, V.G., 1979. Instabilities in Dynamical Systems: Applications to Celestial Mechanics. 1st Edn., D. Reidel Pub. Co., Dordrecht, ISBN: 9027709734, pp: 314.

Truesdale, N., (2012) Using Invariant Manifolds of the Sun-Earth L2 Point for Asteroid Mining Operations, ASEN 5050 Spaceflight Dynamics 12/19/2012.

Yan H. (2020), Port-Hamiltonian Based Control of the Sun-Earth 3D Circular Restricted Three-Body Problem: Stabilization of the L1 Lagrange Point. Modern Mechanical Engineering, 2020, 10, 39-49. https://doi.org/10.4236/mme.2020.103005.

Zeidler E., (1990). Nonlinear Functional Analysis and Its Applications. ISBN 978-1-4612-6971-7 ISBN 978-1-4612-0985-0 (eBook) DOI 10.1007/978-1-4612-0985-0.

Zotos E., E., (2015). How does the oblateness coefficient influence the nature of orbits in the restricted three-body problem? arXiv:1508.05209v1 [astro-ph.EP].